LHCb-PUB-2019-001
February 28, 2019

Luminosity scenarios for LHCb Upgrade II

J. Albrecht[1], M. Charles[2], L. Dufour[3], M. Needham[4], C. Parkes[3,5], G. Passaleva[3,6], A. Schopper[3], E. Thomas[3], V. Vagnoni[7], M. Williams[5], G. Wilkinson[8].

[1] *Technische Universität Dortmund, Dortmund, Germany*
[2] *LPNHE, Sorbonne Université, Paris, France*
[3] *CERN, Geneva, Switzerland*
[4] *University of Edinburgh, Edinburgh, UK*
[5] *University of Manchester, Manchester, UK* [6] *INFN Sezione di Firenze, Firenze, Italy*
[7] *INFN Sezione di Bologna, Bologna, Italy*
[8] *University of Oxford, Oxford, UK*

Abstract

The potential HL-LHC operational scenarios for LHCb Upgrade II are reviewed. Their impact on the physics performance of the LHCb Upgrade II experiment is described considering: the total integrated luminosity to be collected; the impact of beam-crossing angles on measurements of *CP* violation; the effects of pile-up and the size of the luminous region. A maximum instantaneous luminosity of 1.5×10^{34} cm^{-2}s^{-1} is recommended and detectors should be designed to withstand up to 350 fb^{-1} during Run 5 and 6 (400 fb^{-1} in Run 1-6). The RMS of the luminous region, spatially and temporally, should be maximised. Identical crossing angles for both magnet polarities is preferred as is collection of equal integrated luminosity in each configuration. From the scenarios currently presented, a purely vertical crossing plane during collisions best meets these requirements.

1 Introduction

The potential for the HL-LHC to deliver the luminosity required by LHCb Upgrade II has been studied and documented in a CERN accelerator note [1]. The development of these studies was presented on several occasions to the LHCb Collaboration, with a final presentation at the LHCb week in June 2018 [2] and input requested from the collaboration. The studies were considered by the Upgrade II planning group and this note provides our recommendations for a baseline operational scenario. The choice of this baseline is made to allow more detailed studies for the HL-LHC to commence, and to provide input to the detector design studies.

The HL-LHC baseline design [3] is compatible with LHCb running at the Upgrade I luminosity of $2 \times 10^{33} \mathrm{cm}^{-2}\mathrm{s}^{-1}$. Running above the nominal Upgrade I luminosity requires modifications to the HL-LHC optics and layout in the LHCb Insertion Region (IR 8).

The luminosity performance achievable at LHCb for Upgrade II, and the impact on the integrated luminosity in ATLAS and CMS has been studied. The modifications required to the machine layout have also been investigated. These preliminary studies and beam dynamics simulations have shown no fundamental limitations to the delivery of an integrated luminosity of $\sim 50\,\mathrm{fb}^{-1}$ per year at LHCb. They show a corresponding reduction of the integrated luminosity in ATLAS and CMS of less than 3% as a result of the additional burn-off. The CERN accelerator note [1] concludes that "preliminary investigations have identified a range of potential solutions for operating LHCb Upgrade II at a luminosity of up to $2 \times 10^{34} \mathrm{cm}^{-2}\mathrm{s}^{-1}$ and permitting the collection of $300\,\mathrm{fb}^{-1}$ or more at IP8 during the envisaged lifetime of the LHC".

1.1 Prospects for running LHCb at high luminosity

For fixed values of the HL-LHC beam parameters (number of bunches, filling scheme, bunch population, bunch length, transverse emittance) the luminosity delivered at LHCb will essentially depend on the minimum β^* and crossing angles achievable at the interaction point. [1]. LHCb physics will benefit from maximising the RMS of the luminous region, both in space and time, as discussed in Sect. 4.

The minimum β^* and crossing angle are constrained by available magnet strength, beam-beam effects, and aperture considerations. A possible set of HL-LHC compatible parameters have been identified and are listed in Tables 1 and 2 together with the corresponding luminosity performance, under the assumption that the beam lifetime is dominated by burn-off.

All the Upgrade II scenarios proposed in Tables 1 and 2 are based on similar layouts. Operation at high luminosity and with small β^* will enhance beam-beam effects, which could have the potential to reduce the dynamic aperture and therefore lower the integrated luminosities from the values given in the tables, and also degrade the performance at ATLAS and CMS. Detailed simulations, benefiting from the ever-increasing knowledge of the performance of the current machine, are underway to answer these questions [4, 5].

In the scenarios where the beams cross in the horizontal plane, the spectrometer dipole adds an internal crossing angle to the external one [6] resulting in different crossing angles for both magnet polarities. Consequently, the performance differs between the two magnet polarities. Collecting significant samples with both magnet polarities is

[1]The crossing angle is defined as the full angle between the two nominal directions at LHCb.

Table 1: HL-LHC parameters and Luminosity Scenario at LHCb, with different leveled luminosities and dipole polarities for a horizontal crossing plane. The values provided assume standard HL-LHC beams parameters and duty cycle. This table is based on Ref. [1] where full details are provided. The yearly integrated luminosity for ATLAS/CMS during Upgrade I LHCb operations is estimated to be 261.5 fb^{-1}/y.

Parameter	**Unit**	**Lumi scenario**			
Target leveled lumi	$10^{34}\,\text{cm}^{-2}\text{s}^{-1}$	**1.0**		**2.0**	
β^*	m	1.5	1.5	1.5	1.5
Crossing plane		H		H	
Magnet polarity		$-$	$+$	$-$	$+$
External crossing angle	μrad	400	300	400	300
Crossing angle at IP	μrad	130	570	130	570
Virtual (Peak) luminosity	$10^{34}\,\text{cm}^{-2}\text{s}^{-1}$	2.16	1.57	2.16	1.57
Leveled pile-up	1	28	28	56	44.2
Long. RMS luminous region (start)	mm	52.7	39.5	52.7	39.5
Peak line pile-up density (start)	mm^{-1}	0.20	0.28	0.41	0.44
Eff. line pile-up density (start)	mm^{-1}	0.13	0.17	0.20	0.20
Fill duration	h	8.0	8.0	7.7	8.0
Leveling time	h	4.7	3.1	0.6	0
Integ. lumi. at LHCb	fb^{-1}/y	**46.3**	**40.9**	**61.7**	**46.2**
Integ. lumi. at ATLAS/CMS	fb^{-1}/y	257.1	257.7	255.1	257.0

desirable for the LHCb physics programme, as it simplifies the study of some sources of systematic uncertainties in *CP*-violation measurements (further discussed in Sect. 3). Injecting the beams with vertical crossing angles is not possible at IP8 because of aperture limitations from the beam screens. However, a vertical crossing plane can be implemented: a horizontal crossing angle can be used at injection and the crossing plane can be rotated before establishing collisions in LHCb. Indeed, a similar scheme has already been used in operation in 2012, but it adds significant operational complexity and beam dynamics constraints. The vertical crossing allows identical interaction point (IP) characteristics (Luminosity, pile-up, and size of the beam spot) for each detector magnet polarity to be achieved. However, the maximum integrated luminosity at LHCb will be achieved by running with a horizontal crossing angle and without magnet-polarity reversal. Additional scenarios based on flat optics ($\beta^*_{\text{y}} < \beta^*_{\text{x}}$) could be considered to overcome some of the aperture limitations and further increase the luminosity [5] but they have not been studied yet.

1.2 Energy deposition and shielding issues

A simulation of the LHC machine layout around LHCb, using the Fluka package [8], was performed in order to assess the energy deposition in the different machine components [1]. This study and its conclusions were already outlined in the Upgrade II Expression of Interest in 2017 [9]. As a large crossing angle (770 μrad) in the horizontal plane was pessimistically assumed at that time, the conclusions remain valid for the new scenarios presented in this document. In order to operate at high luminosity, additional elements

Table 2: HL-LHC parameters and Luminosity Scenario at LHCb, with different leveled luminosities and dipole polarities for a vertical crossing plane. The values provided assume standard HL-LHC beams parameters and duty cycle. This table is based on Ref. [1] and [7] where full details are provided. The yearly integrated luminosity for ATLAS/CMS during Upgrade I LHCb operations is estimated to be 261.5 fb^{-1}/y.

Parameter	**Unit**	**Lumi scenario**		
Target leveled lumi	$10^{34}\,\mathrm{cm}^{-2}\mathrm{s}^{-1}$	**1.0**	**1.5**	**2.0**
β^*	m	1.5	1.5	1.5
Crossing plane		V	V	V
Magnet polarity		$\pm$	$\pm$	$\pm$
External crossing angle	μrad	320	320	320
Crossing angle at IP	μrad	419	419	419
Virtual (Peak) luminosity	$10^{34}\,\mathrm{cm}^{-2}\mathrm{s}^{-1}$	1.79	1.79	1.79
Leveled pile-up		28	42	50.3
Long. RMS luminous region (start)	mm	44.7	44.7	44.7
Peak line pile-up density (start)	mm^{-1}	0.25	0.37	0.44
Eff. line pile-up density (start)	mm^{-1}	0.15	0.20	0.20
RMS luminous time (start)	ns	0.186	0.186	0.186
Peak time pile-up density (start)	ns^{-1}	21.2	21.2	21.2
Fill duration	h	8.0	-	7.9
Leveling time	h	3.6	1.3	0
Integ. lumi. at LHCb	fb^{-1}/y	**42.5**	**49.9**	**51.0**
Integ. lumi. at ATLAS/CMS	fb^{-1}/y	257.5	-	256.4

will be added to the machine layout at each side of the LHCb IP, in particular:

- a TAS (Target Absorber) to protect the inner triplet from quenching, and to limit its radiation dose,
- a TAN (Target Absorber Neutrals) to shield the recombination dipoles D2 from high-energy neutral particles,
- and a TCL (Target Collimator Long) to protect the cold magnets in the matching sections from collision debris.

Additional items could still be required and the cost and installation work related to raising the LHCb luminosity for Upgrade II are being investigated. A mini-TAN will already be installed during LS2 to allow for $2 \times 10^{33}\,\mathrm{cm}^{-2}\mathrm{s}^{-1}$ operation. Thanks to its effective final design and location it is possible that this could also suffice for the higher luminosity conditions of Upgrade II, though this has still to be fully proven.

The lifetime of the triplet quadrupoles at LHCb is assumed to be identical to that of the triplets currently in place at the high luminosity IPs. They are designed to withstand a dose of 30MGy, corresponding to $300\,\mathrm{fb}^{-1}$ at the IP of ATLAS. Further energy deposition studies will allow the design and the crossing angle scheme at LHCb to be optimised and consequently potentially to extend the lifetime of the quadrupoles beyond that limit. The existing triplets at ATLAS and CMS will be removed in LS3. A careful inspection of these triplets after removal will also shed light on the radiation hardness of these components and the possibility of running beyond their currently accepted lifetime. Conservatively, $300\,\text{fb}^{-1}$ of integrated luminosity for the LHCb Upgrade II has been assumed for the physics projections reported in the Upgrade II physics case [10]. The maximum likely collected integrated luminosity is an important parameter for the detector design, and this is considered in Sect. 2.

2 Integrated luminosity considerations

LHCb Upgrade II aims to bring the total data collected by LHCb to $300\,\text{fb}^{-1}$ or more. This requires the collection of 250 fb^{-1} or more during Run 5 & 6 of the LHC, with an annual collected luminosity of approximately $50\,\text{fb}^{-1}$. Naturally, at this stage the detailed schedule is not yet known with a high degree of confidence. The most common assumption has typically been two runs each of three years, separated by a one year technical stop. The current LHC schedule, shown in Fig. 1, assumes Run 5 is three years long and Run 6 is four years.

The predictions for LHCb use the standard HL-LHC operational scenario in Refs. [11,12] where 160 proton-proton physics collision days/year is assumed; it is foreseen by the accelerator division that this number is conservative and will increase as they assume there will be fewer special runs, notably ion running, and less machine development than currently.

The primary installation of LHCb Upgrade II will be during LS4, with preparatory work being carried out during LS3. Consequently we assume only half the standard annual integrated luminosity is collected in the first year of operations due to experimental commissioning. Table 3 gives integrated luminosities in the LHCb favoured vertical crossing scheme at three target leveled luminosities (as given in table 2). Note that in the target leveled luminosity of $2.0 \times 10^{34}\text{cm}^{-2}\text{s}^{-1}$ scenario the actual virtual (peak) luminosity is below this value reaching only $1.79 \times 10^{34}\text{cm}^{-2}\text{s}^{-1}$. In all cases the levelling time does not exceed a few hours.

The maximum instantaneous luminosity scenario is disfavoured by the machine as it pushes parameters to their limits and increases the pile-up and occupancy that must be accommodated by the experiment design for a relatively modest gain in luminosity compared with the second scenario. The lowest instantaneous luminosity scenario may achieve the target $300\,\text{fb}^{-1}$ only with seven years of operation across Run 5 and 6. Consequently we select the middle scenario of a maximum levelled luminosity of $1.5 \times 10^{34}\text{cm}^{-2}\text{s}^{-1}$ as the baseline. The anticipated total luminosity (Run1–6) collected by LHCb with this baseline is thus in the range 300–350 fb^{-1}. As the integrated luminosity may be limited by the triplet quadruples (see Sect. 1.2), we retain $300\,\text{fb}^{-1}$ as the assumption for all physics projections. Due to the potentially conservative assumption on the number of operating days, machine availability, and the possibility at this stage of additional years being added to Run 5 and 6 (each additional year adding $\sim 50\,\text{fb}^{-1}$) we would propose that the detector and machine consider designs that allow the possibility of collecting up to $400\,\text{fb}^{-1}$ in total (Run 1–6), *i.e.* of $350\,\text{fb}^{-1}$ in Run 5 and 6.

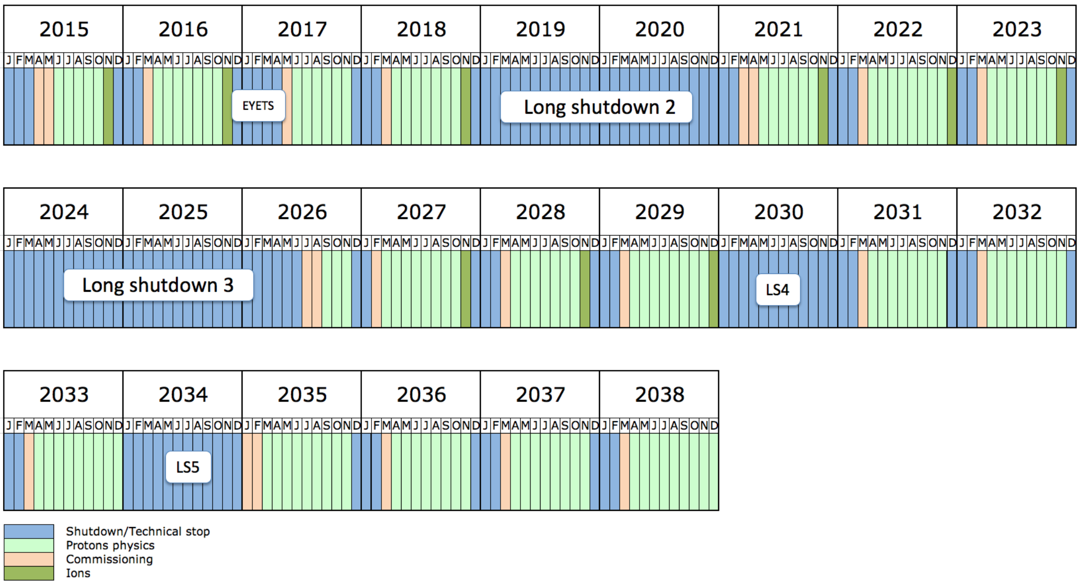

Figure 1: Current version of the LHC and HL-LHC operational schedule. Reproduced from [13].

Table 3: Integrated Luminosity to be collected at LHCb by the end of LHC Run 6. Values are given assuming three or four years of operations in Run 6. All values assume the vertical crossing scenario and numbers are given for three targets of levelled instantaneous luminosity.

LHC Run Year	**Integrated Luminosity fb^{-1}**		
	$1 \times 10^{34}\mathrm{cm}^{-2}\mathrm{s}^{-1}$	$1.5 \times 10^{34}\mathrm{cm}^{-2}\mathrm{s}^{-1}$	$2.0 \times 10^{34}\mathrm{cm}^{-2}\mathrm{s}^{-1}$
Run 1-4	50	50	50
LS4	-	-	-
Run 5 Year 1	21	25	26
Run 5 Year 2	43	50	51
Run 5 Year 3	43	50	51
LS5	-	-	-
Run 6 Year 1	43	50	51
Run 6 Year 2	43	50	51
Run 6 Year 3	43	50	51
Total	**284**	**325**	**331**
Run 6 Year 4	43	50	51
Total	**326**	**374**	**381**

3 Impact of beam-crossing angles on detector acceptance

As a result of the beam-crossing angle, particles produced in the pp collision are not centred along the z axis of the LHCb coordinate system. In particular, a crossing in the horizontal direction (as defined in the LHCb coordinate system) leads to a left-right asymmetry in the momentum distribution of the produced particles. By the design of the LHCb spectrometer, this initial direction affects the geometrical acceptance for charged particles differently, depending on the charge of the particle [14]. This effect is most prominent for charged particles which travel close to the beam-pipe, i.e. those with a high pseudorapidity, for which the influence of the horizontal crossing angle is illustrated schematically in Fig. 2. Therefore, to estimate the effects of the proposed beam-crossing scenarios, the effect on the detection asymmetry for muons at high pseudorapidities is considered. The phase-space of muons generated in decays of the type $B^+ \to J/\psi\,(\to \mu^+\mu^-)K^+$ are used. Analyses performed in bins of rapidity, such as measurements of production asymmetries, are particularly sensitive to the detection asymmetry at a high pseudorapidity. Extrapolating the statistical uncertainties of the measurement of the B^+ production asymmetry [15] to $300\,\mathrm{fb}^{-1}$, shows that effects of $\mathcal{O}(0.05\%)$ will already require a suitable calibration. While calibrations of the instrumental asymmetries exist, it is desirable to reduce the size of these corrections to account for unforeseen effects and shortcomings in their treatment. In this Section, the order-of-magnitude of the introduced instrumental asymmetries are discussed.

As a rule-of-thumb, the detection asymmetry introduced by the beam-crossing angles are mitigated significantly when: 1. the crossing angles are identical for both magnet polarities, both in magnitude and in sign and 2. the data sets of opposite magnet polarities are averaged. This requirement applies to the crossing angle resulting from the sum of the internal and external one. Note that, to achieve this, a horizontal component must be present in the external crossing angle to appropriately cancel the effect of the internal crossing angle.

3.1 Event generation and simplified detector simulation

To generate a sufficiently large data sample to see the influence of $\mathcal{O}(0.1\%)$ asymmetries, a fast simulation technique is used. B^+ mesons are generated and propagated through the detector material using the particle-gun mode of GAUSS. The distribution of the transverse momentum, p_{T}, and pseudorapidity, η, of the B^+ mesons are extracted from simulated $\sqrt{s} = 14\,\mathrm{TeV}$ proton-proton collisions modelled by PYTHIA. Finally, The angular distribution in the p_y, p_x plane is modified to account for the small, additional, boost in the x-direction, as introduced by the beam-crossing angle.

The simulation of interactions of the final-state particles with the detector material, as done in GEANT4, is time consuming. Meanwhile, the beam-crossing angle affects particles primarily through a change in the geometrical acceptance. Its effects are therefore estimated using a simplified event simulation. In this simulation, charged particles are transported numerically from its origin vertex through the LHCb detector, without accounting for material interactions such as multiple scattering. A particle is considered to be in acceptance if sufficient sensitive detector layers were traversed. Here, the definition for long tracks is employed, meaning that the particles must traverse sufficient VELO sensors and layers of the T-stations,

$$\varepsilon = \frac{N(3\text{ VELO }\phi,\, r\text{ hits \& 3 T-station }X,\text{ stereo hits})}{N(\text{Generated})}.$$

The detection asymmetry, A_{det}, is defined as the relative difference in efficiency between the opposite charges,

$$A_{\mathrm{det}} = \frac{\varepsilon^+ - \varepsilon^-}{\varepsilon^+ + \varepsilon^-}.$$

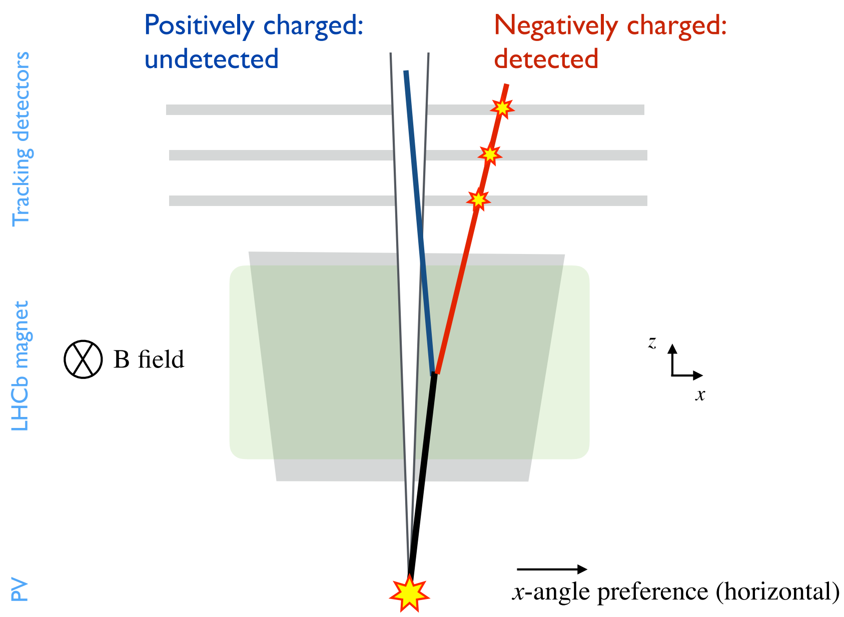

Figure 2: Simplified schematic view of the LHCb detector, along with the impact of the deflection of the magnetic field on charged particles, using the LHCb coordinate system.

This model has been used successfully in a description of the detection asymmetry of muons [14].

3.2 Results

Figure 3 shows the simulated detection asymmetry for a purely vertical crossing scenario ($\theta_y = 419\,\mu$rad, $\theta_x = 0$), and that of the horizontal beam-crossing with the highest luminosity in Table 1, $\theta_x = -130\,\mu$rad for magnet up and $\theta_x = -570\,\mu$rad for magnet down, where θ_x (θ_y) is the horizontal crossing angle in LHCb's $x - z$ ($y - z$) plane. No asymmetry in the geometrical acceptance is observed for a purely vertical crossing scenario. However, an asymmetry for the scenario with the highest luminosity is visible for $\eta \geq 4.7$, showing that the cancellation of the asymmetries originating from the crossing angle is not ensured.

4 Impact of beam-crossing angles on detector performances

At a fixed instantaneous luminosity, changing the beam crossing angle will change the size of the luminous region (in both longitudinal and transverse directions). In this section we show that this leads directly to changes in the event reconstruction performance (in track reconstruction, and PV association). As such, the recommendation is to use a scheme with identical crossing angles for the two magnet polarities. Furthermore, the performance is in general improved for a larger luminous region, all other factors being equal, so a secondary recommendation is to maximise the extent of the pile-up region in space and time.

4.1 Particle tracks reconstruction

In addition to the asymmetry introduced by the geometrical acceptance of the detector, the high-luminosity scenario also involves a significantly different pile-up (and hence detector occupancy) between the two magnet polarities. The performance of the current reconstruction algorithms decreases as detector occupancy rises. While the optimisation of these algorithms is a prerequisite for the very different expected conditions, the dependence of their performance on the detector occupancy is still expected. Meanwhile, the quality of a reconstructed track also depends on the encountered material along this trajectory, as small (large) kinks occur due to elastic (hadronic) scattering. The effective thickness of the encountered material differs between the charges. Therefore, also the quality of the reconstructed tracks differs.

In Ref. [14] it is shown that, at higher hit multiplicities, the charge asymmetry in the performance of the track reconstruction increases (for particles with $p \leq 10\,\mathrm{GeV}/c$), up to $\mathcal{O}(0.5\%)$ for moderately high occupancies. This result is consistent with an increase in difference in track quality between the charges. By construction, this effect is reduced when the data sets of different magnet polarities, but same hit multiplicities, are averaged. Dealing with significant differences in the detector occupancy between the polarities will be a delicate task in the development of the track reconstruction.

4.2 Primary Vertex association

An important design consideration for any future LHCb upgrade will be the ability to accurately reconstruct long-lived particles, and associate them with the primary interaction vertex (PV) from which they originated. In this section a generic b hadron is used by way of example, but the same arguments apply for c hadrons. If a b hadron is mistakenly associated with a PV from which it did not originate, the measured decay time of the particle will be incorrect. This will lead to additional systematic uncertainties for any decay-time-dependent analyses, including searches for, and characterisation of, *CP* violation in meson-antimeson oscillations.

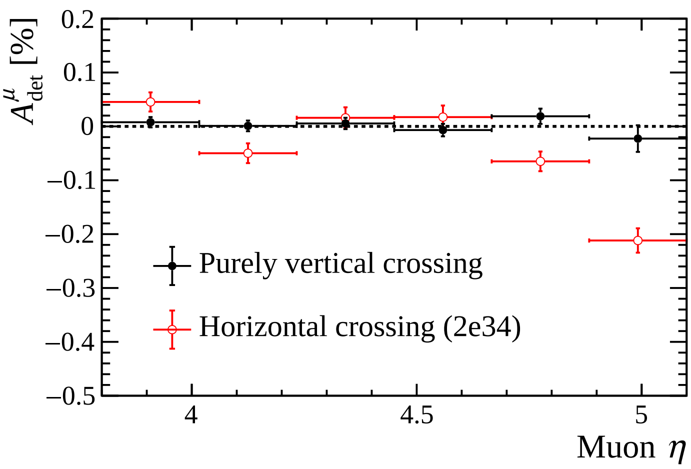

Figure 3: Expected magnet-averaged detection asymmetry due to the geometrical acceptance only, for two different beam-crossing scenarios.

In particular, if the PV association performance differs between the two magnet polarities of the LHCb dipole magnet, the cancellation of instrumental asymmetries by averaging over the two polarities will be inherently limited, in ways that may be challenging to determine and quantify.

At the high luminosity conditions considered in this document, the mean number of PVs will range from 28 (for L= 1×10^{34} cm^{-2}s^{-1}) to 55 (for L= 2×10^{34} cm^{-2}s^{-1}), distributed in space and time according to the details of the collision environment. For a fully-reconstructed b hadron, the position of its decay vertex (also referred to as the secondary vertex, SV) and the final-state particle momenta allow the b hadron to be extrapolated back into the luminous region to identify the source PV from spatial information alone. In addition, time information will be available for hits in the vertex detector in Upgrade II, which will allow temporal PV matching and significantly improve the matching efficiency. Matching in time may be incorpotated in other areas of the detector, notably in the ECAL for neutral particles.

The rate of PV misassociation will depend in general on the precision of the positions and times of primary and secondary vertices, and on the final-state particle momentum resolution. However, the PV association is also strongly dependent on the size of the luminous region in space (both longitudinally and in the transverse plane) and time. To quantify this dependence a simple simulation has been developed, briefly described in this section.

In brief, primary interaction vertices are first generated in (x,y,z,t) under a range of different scenarios for the luminous region and instantaneous luminosity. Charged particles are generated from each of these PVs according to known kinematic and multiplicity distributions from full simulation. From one PV a B^0 meson is generated (again with kinematics sampled from full simulation), and allowed to travel and decay exponentially into a $\pi^+\pi^-$ final state. All charged particles are then propagated through a vertex detector model, with a geometry based on the Upgrade-I VELO and with realistic hit precision, and tracks and vertices are reconstructed under some reasonable requirements on the number of hits (for tracks) and number of tracks (for vertices). Finally, the reconstructed spatial and temporal information is used to select the best candidate PV for the B^0 meson. The results presented here assume a VELO detector with $55 \times 55 \mu\text{m}^2$ pixels, and a single-hit time precision of 200 ps or better.

The figure-of-merit from this study is the PV misassociation fraction, which is calculated under different assumptions about the availability and precision of time information for the VELO hits. Different hit time precisions are considered for the inner ($5 < r < 20$ mm) and outer ($20 < r < 35$ mm) radial regions of the detector, to account for the different radiation and occupancy conditions. For the purposes of this note the results and discussion are limited to the influence of the crossing angle and size of the luminous region. As a reference, the anticipated PV misassociation fraction under Run 3 conditions is of order 1%. While it is difficult to sustain this performance under 5–10 times higher luminosities, we should aim to stay as close as possible to this benchmark.

As can be seen in Tables 1,2, the longitudinal RMS of the luminous region is strongly dependent on the crossing angle. Figure 4 shows the PV misassociation fraction under two different crossing angles, at a given value of instantaneous luminosity and β^*. This study was performed using a previous set of beam parameters to those presented in Tables 1,2, but the general conclusions are independent of the details. For a larger crossing angle, the PV matching performance is worse, as a consequence of the longitudinal compression

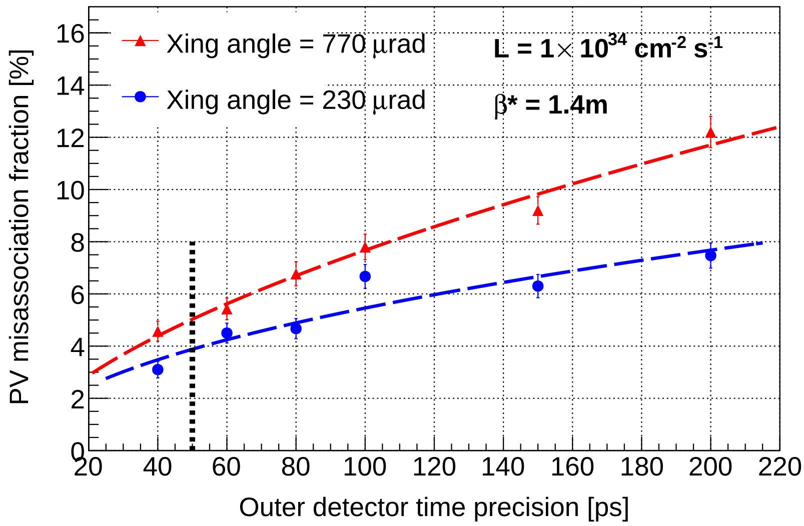

Figure 4: PV misassociation fraction for $B^0 \to \pi^+\pi^-$ decays under different crossing angle values. The results are plotted as a function of the time precision on hits in the vertex locator, where realistic scenarios are to the right of the vertical dashed line. For this plot, no time information is assumed for the inner detector. These studies predate the scenarios shown in Tables 1 and 2. The (x,y,z,t) RMS values for the pile-up region are (15.3μm,15.3μm,51.9mm,190ps) for for a crossing angle of 230 μrad, and (15.3μm,15.3μm,32.7mm,202ps) for 770 μrad.

of the luminous region. In this study this RMS is 51.9 mm (32.7 mm) for a crossing angle of 230 μrad (770 μrad). The results show that, in this realm of detector performance and collision environment, the PV misassociation fraction scales approximately linearly with the longitudinal RMS of the luminous region.

Similarly, the transverse RMS of the luminous region will influence the PV association performance. Figure 5 shows the corresponding performance plot for a (deliberately wide) range of values for the transverse RMS. The dependence is weaker than that observed for the longitudinal RMS, largely because the longitudinal separation of PVs is significantly more important than the transverse separation when performing the matching for long-lived particles. Nevertheless, all other things being equal, the performance is improved with a larger transverse RMS.

Given the significant change in PV association performance driven by changes in the size of the luminous region, a principle conclusion of this study is that the crossing angle (and other beam parameters) should if possible be identical under the two LHCb dipole magnet polarities, and stable over time. The second conclusion is that for a given instantaneous luminosity the RMS of the luminous region should be maximised in both time and space (including both longitidinal and transverse components).

5 Summary

This impact of the proposed HL-LHC operational scenarios on the physics performance of Upgrade II has been considered. Operating at a maximum instantaneous luminosity of $1.5 \times 10^{34}\text{cm}^{-2}\text{s}^{-1}$ is recommended. This is a compromise between collecting the maximum data sample in the available HL-LHC schedule and detector and accelerator

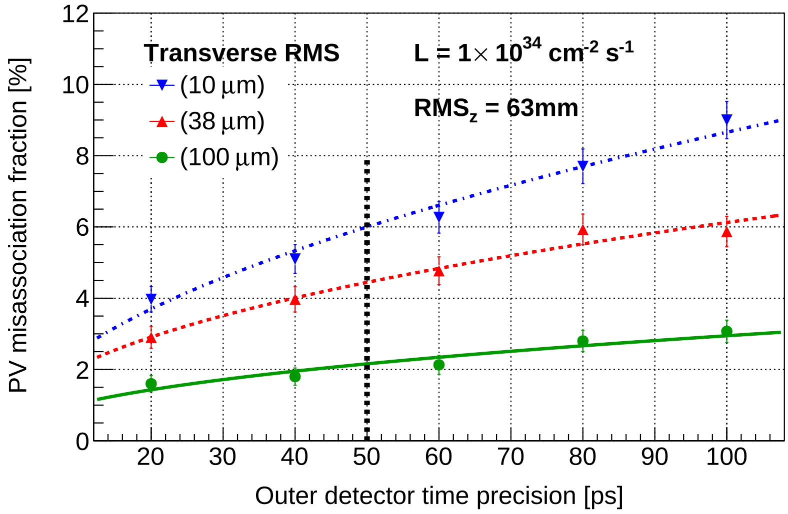

Figure 5: PV misassociation fraction for $B^0 \to \pi^+\pi^-$ decays under different values for the transverse RMS of the luminous region (with longitudinal RMS fixed at $\sigma_z = 63\,\text{mm}$). The results are plotted as a function of the time precision on hits in the vertex locator, where the most realistic scenarios are to the right of the vertical dashed line. For this plot, no time information is assumed for the inner detector.

design considerations.

We anticipate the collection of a total LHCb (Run 1–6) data sample of at least 300 fb^{-1} (250 fb^{-1} Run 5–6), and this value should be used for physics projections. Uncertainties on the schedule and operational parameters mean that a total LHCb sample of up to 400 fb^{-1} (350 fb^{-1} Run 5–6) is possible, and this value should be used for safety when considering radiation requirements in detector designs. The maximum integrated luminosity may be limited by the radiation tolerance of the inner triplet quadrupoles and this will need to be studied. We understand that a full evaluation may not be possible until the quadrupoles of ATLAS and CMS are removed in LS3.

The vertex detector of LHCb identifies the primary vertex at which the proton-proton collision occurs and the secondary decay vertex of the heavy-flavour hadron which must be associated to the correct primary vertex. The electromagnetic calorimeter must also associate photons and π^0 to the correct vertex. At the higher pile-up of Upgrade II a new innovation will be using time measurements as well as spatial measurements to perform this. Consequently, the RMS of the luminous region, spatially and temporally, should be maximised.

A core element of the LHCb physics programme is the study of *CP* violation. The detector calibration, required to perform such measurements, benefits from cancellations between the two magnet polarities, as they simplify studies of systematics. This benefits from the collection of relatively equal integrated luminosities with both magnet polarities, such that the most similar conditions possible for the two polarities are obtained. Ideally, the beams would cross with the same angle (magnitude and sign) for both magnet polarities. If this were not possible, the same crossing angle magnitude for both polarities would be preferred. The horizontal component of the crossing angle should be minimized. More generally, the RMS of the luminous region in time and space should if possible be identical between magnet polarities.

Considering the scenarios currently presented, using a vertical crossing plane during collisions best meets these requirements. However, we remain open to any solution that best meets the requirements discussed here.

More advanced studies of the operational machine scenarios and the required designs for the additional machine elements for this programme will be needed on the timescale of the LHCb Upgrade II technical design report in two years. While the detailed schedule of LS4 cannot be known at this stage, it is clear that the extended duration of LS3 gives excellent opportunities for preparatory work for Upgrade II on both the detector and machine sides. We encourage consideration of what work can be performed in advance in LS3.

6 Acknowledgements

We would like to thank Federico Alessio and Massimiliano Ferro-Luzzi for reviewing this note. The LHCb Collaboration would like to thank the HL-LHC machine team and in particular all authors of Ref. [1] and Luis Eduardo Medina Medrano for useful discussions. We have enjoyed a very profitable exchange of information with them and their preliminary studies were central to the LHCC recently approving that LHCb Upgrade II proceeds to a technical design report.

References

[1] I. Efthymiopoulos *et al.*, *LHCb Upgrades and operation at* $10^{34}\,\mathrm{cm}^{-2}\mathrm{s}^{-1}$ *luminosity — A first study*, Tech. Rep. CERN-ACC-NOTE-2018-0038, May, 2018.

[2] B. Di Girolamo and I. Efthymiopoulos, *Report from HL-LHC*, https://indico.cern.ch/event/672225/contributions/3022146/attachments/1667159/2673176/LHCbU HLLHC-BDGIE-20180613.pdf, 2018.

[3] G. Apolinari *et al.*, *High-Luminosity Large Hadron Collider (HL-LHC) : Technical Design Report V. 0.1*, CERN-2017-007-M. doi: 10.23731/CYRM-2017-004.

[4] Y. Papaphilippou, *Operation with high luminosity LHCb*, 26th LARP Hi-Lumi Collabora-tion Meeting, SLAC, USA, May, 2016.

[5] R. De Maria *et al.*, *HL-LHC operations with LHCb at high luminosity*, 3^{rd} Workshop on LHCb Upgrade II, Annecy, France, March 21-23, 2018.

[6] W. Herr and Y. Papaphilippou, *Alternative running scenarios for the LHCb experiment*, Tech. Rep. LHC-PROJECT-Report-1009, CERN, Geneva, Jan, 2007.

[7] L. E. Medina Medrano, *Private Communication*, Thesis in preparation, 2018.

[8] T. T. Bhlen *et al.*, *The FLUKA Code: Developments and Challenges for High Energy and Medical Applications*, Nucl. Data Sheets **120** (2014) 211.

[9] LHCb collaboration, *Expression of Interest for a Phase-II LHCb Upgrade: Opportunities in flavour physics, and beyond, in the HL-LHC era*, CERN-LHCC-2017-003.

[10] LHCb collaboration, *Physics case for an LHCb Upgrade II — Opportunities in flavour physics, and beyond, in the HL-LHC era*, `arXiv:1808.08865`.

[11] E. Metral *et al.*, *Update of the HL-LHC operational scenarios for proton operation*, Tech. Rep. CERN-ACC-NOTE-2018-002, Jan, 2018.

[12] L. E. Medina Medrano, R. Tomas Garcia, G. Arduini, and M. Napsuciale, *Effective pile-up density as a measure of the experimental data quality for High-Luminosity LHC operational scenarios*, Tech. Rep. CERN-ACC-NOTE-2018-003, Jan, 2018.

[13] HL-LHC Collaboration, *LHC Schedule*, https://lhc-commissioning.web.cern.ch/lhc-commissioning/schedule/images/schedule-to-2038.png, 2018.

[14] L. Dufour and J. Van Tilburg, *Decomposition of simulated detection asymmetries in LHCb*, Tech. Rep. LHCb-INT-2018-006. CERN-LHCb-INT-2018-006, CERN, Geneva, Feb, 2018.

[15] LHCb collaboration, R. Aaij *et al.*, *Measurement of the $B^{\pm}$ production asymmetry and the CP asymmetry in $B^{\pm} \to J/\psi K^{\pm}$ decays*, Phys. Rev. **D95** (2017) 052005, `arXiv:1701.05501`.